Thermal performance of fish is explained by an interplay between physiology, behaviour, and ecology

Philipp Neubauer[1,*]

Ken H. Andersen[2]

1. Dragonfly Data Science, PO Box 27535, Wellington 6141, New Zealand;

2. Centre for Ocean Life, National Institute of Aquatic Resources, Technical University of Denmark, 7 Kemitorvet B 202, 2800 Kongens Lyngby, Denmark;

* Corresponding author's contact:

email: neubauer.phil@gmail.com Tel: +64 4 385 9285

Summary: Although a number of theories exist, there is currently little consensus on drivers of thermal performance in ectotherms, and fish in particular. We present a general size and trait based model that shows that thermal performance can be explained by an interplay of physiological, ecological, and behavioural constraints.

Abstract

Increasing temperatures under climate change are thought to affect individual physiology of fish and other ectotherms through increases in metabolic demands, leading to changes in species performance with concomitant effects on species ecology. Although intuitively appealing, the driving mechanism behind thermal performance is contested: thermal performance (e.g., growth) appears correlated with metabolic scope (i.e., oxygen availability for activity) for a number of species, but a substantial number of datasets do not support oxygen limitation of long-term performance. Whether or not oxygen limitations via the metabolic scope, or a lack thereof, have major ecological consequences remains a highly contested question. Here, we propose a general size and trait-based model of energy and oxygen budgets to determine the relative influence of metabolic rates, oxygen limitation, and environmental conditions on ecotherm performance. We show that oxygen limitation is not necessary to explain performance variation with temperature. Oxygen can drastically limit performance and fitness, especially at temperature extremes, but changes in thermal performance are primarily driven by the interplay between changing metabolic rates and species ecology. Furthermore, our model reveals that fitness trends with temperature can oppose trends in growth, suggesting a potential explanation for the paradox that species often occur at lower temperatures than their growth-optimum. Our model provides a mechanistic underpinning that can provide general and realistic predictions about temperature impacts on the performance of fish and other ectotherms, and function as a null model for contrasting temperature impacts on species with different metabolic and ecological traits.

Keywords: thermal performance, OCLTT, metabolic rate, climate change

2

Introduction

Temperature, through its effects on individual physiology, is a dominant driver of species ecology and bio-geography (Deutsch et al. 2015; Pinsky et al. 2013). As a consequence, current and predicted temperature increases under climate change will act as a strong agent of change in many ecosystems (Deutsch et al. 2015; Parmesan and Yohe 2003; Stuart-Smith et al. 2015; Walther et al. 2002). However, the nature of these changes can be difficult to predict as temperature effects scale from individuals to species and ecosystems. Through this cascade of scales, incorrect or approximate model assumptions at the individual scale can have disproportionate effects on ecosystem level outcomes (Brander et al. 2013; Lefevre et al. 2017). In marine fish, for example, recent predictions of decreasing organism size, and resulting decreases in the size of fisheries catches (Cheung et al. 2013), have been criticized as overly simplistic and not in line with physiological constraints (Brander et al. 2013; Jutfelt et al. 2018; Lefevre et al. 2017).

Although there are conceptual and model frameworks to explain aspects of thermal performance and ecological responses to temperature (Brown et al. 2004; Fry 1947; Pauly and Cheung 2017; Pörtner 2010), many of these remain controversial as they appear limited in their generality or predictive capacity (Jutfelt et al. 2018; Lefevre et al. 2017). To our knowledge, no general theoretical framework exists to quantitatively explain and predict changes in ecological rates, such as observed change in growth and asymptotic size (e.g., the temerature-size rule in ectotherms; Angilletta et al., 2004; Atkinson, 1994)), or attack rates (Englund et al. 2011; Rall et al. 2012) with temperature, from fundamental physiological processes. Instead, and as advocated by the metabolic theory of ecology (Brown et al. 2004), ecological theory often treats ecological rates as being directly temperature dependent, without a direct link to the underlying physiological drivers (e.g., Angilletta et al.,

3

2004; Guiet et al., 2016; Vucic-Pestic et al., 2011).

⁴⁵ A phenomenological description that assumes a general ecological temperature response often fails to explain heterogeneity in ecological responses (Angilletta et al. 2004; Rall et al. 2012). Although ecological rates seem to follow some general patterns in the response to temperature, ⁴⁸ there is also significant heterogeneity between species and trait groups (e.g., Angilletta et al., 2004; Englund et al., 2011; Rall et al., 2012). This leads to difficulties with extrapolation across species or other model components (e.g., fish in marine ecosystem models; Guiet et al., 2016). In ⁵¹ this case, a deeper understanding of the underlying drivers of thermal responses may be necessary in order to derive general predictions about ecological responses to changing temperatures (e.g., Lefevre et al., 2017; Vucic-Pestic et al., 2011). Since the primary effect of temperature of organisms ⁵⁴ is on individual physiology, a general model to explain ecological response should be grounded in physiology.

Physiologically, a long held view has been that temperature is a controlling factor while oxygen ⁵⁷ supply sets the physiological limits (Claireaux and Lefrançois 2007; Fry 1947; Lefevre 2016). How exactly temperature influences ectotherm physiological rates and limits, however, has been a matter of debate, not least because of the variable responses observed among different species. In most ⁶⁰ species, the standard metabolism (SM; the metabolic cost of maintenance and routine activity such as ventilation) increases near exponentially with temperature. A prevalent view is that the maximum metabolic rate (MMR; the metabolic rate at maximum sustained exercise) has a dome- ⁶³ shaped response to temperature, whereby it can be increased (passively and actively) up to a point, but plateaus or decreases thereafter (Claireaux and Lefrançois 2007; Fry 1947; Lefevre 2016; Pörtner and Farrell 2008). This leads to the view of a uni-modal curve for metabolic scope (MMR minus ⁶⁶ SM; the available oxygen/energy for additional activity), and suggests that towards the upper end

4

of this curve, organisms will, simply put, run out of oxygen.

This view was encapsulated in the Theory of Oxygen and Capacity Limitation of Temperature (Pörtner 2010), which suggests that the decrease in metabolic scope towards extreme temperatures limits species ability to sustain core functions such as foraging and growth (i.e., functions beyond SM). In some species, however, maximum metabolic rate increases steadily (Lefevre 2016; Verberk et al. 2016), suggesting that oxygen may not be the limiting factor at high temperatures. Indeed, it has been argued that oxygen is unlikely to determine performance for most species over most of their temperature range as oxygen limits are rarely reached during normal activity (Holt and Jorgensen 2015; Jutfelt et al. 2018).

Here, we propose a general quantitative size- and trait-based eco-physiological model to derive general predictions about temperature impacts on fish physiology, performance and ecology. We describe simple size-dependent physiological processes within an ecological context, and, using a simple optimisation argument, show that observed ecological responses of different life-history strategies can be predicted on the basis of optimised bio-energetics under different temperatures.

Methods

Key assumptions

Our model assumes that physiology is described by two key budgets: the energy and oxygen budgets (Holt and Jorgensen 2014, 2015). We assume that animals will adapt activity levels to optimise available energy for growth and reproduction relative to mortality risk. Available energy is determined either by food capture, food processing capacity, or by available oxygen. We further assume that temperature acts directly on rates that are determined by enzymatic activity: digestive

activity (via maximum consumption) and metabolic costs. Consequently, temperature only acts on ecological rates (e.g., actual feeding rates) via optimisation of activity levels.

Model description

Ectotherms adjust the relative amounts of time (τ) spent on metabolically costly activity and resting/hiding to optimise the net energy gain relative to mortality (Gilliam and Fraser 1987). In the following, we refer to τ as the activity fraction for sake of generality. Since both energy gain and metabolic losses are sensitive to temperature and oxygen limitations, both the activity level and the net energy gain will be subject to these environmental constraints. Their interplay thus determines available energy for growth and reproduction.

Net energy gain P (mass per time) is the difference between supply S and metabolic demands D, each being functions of body weight w and temperature T:

$$P(w, T) = S(w, T) - D(w, T) \tag{1}$$

$$= (1 - \beta - \phi)f(w, T)hc(T)w^q - c(T)kw^n - \tau c(T)k_a w \tag{2}$$

where the feeding level $[0 : 1]$ is given by a Holling type II function response:

$$f(w, T) = \frac{\tau \gamma \Theta w^p}{\tau \gamma \Theta w^p + hc(T)w^q}, \tag{3}$$

where $hc(T)w^q$ is the maximum consumption rate. The feeding level is determined by the fraction of time spent foraging τ (henceforth the activity fraction), foraging rate $\gamma w^p \Theta$ (search rate γw^p times prey availability Θ) and maximum consumption $hc(T)w^q$. The supply is discounted by the loss due to specific dynamic action β (SDA, or heat increment; the energy spent absorbing food), and ϕ is the fraction of food excreted and egested.

6

102   Metabolic demands ($D(w, T)$) are standard metabolism ($\propto kw^n$), which scales with exponent

$n < 1$, and active metabolism $\propto \tau k_a w$, which scales proportional to mass owing to muscular

demands scaling approximately isometrically with weight (Brett 1965; Glazier 2009, and the activity

105 fraction. Temperature scaling of metabolic rates (standard and active metabolism, and maximum

consumption rate) is determined by enzymatic processes (e.g., digestion, glycolysis Jeschke et al.

2002; Sentis et al. 2013) and approimated by an Arrhenious scaling $c(T) = e^{E_a(T-T_0)/(bTT_0)}$, where

108 E_a is the activation energy, assumed constant, T_0 is the reference temperature (here 15 degrees

Celsius), and b is the Bolzman constant. Note that we only scale rates related to enzymatic

activity with temperature, we do assume that ecological rates such as foraging rates or activity

111 are a direct function of temperature. Rather, they are modulated by an individual's behavioural

response to temperature driven physiological changes.

The oxygen budget $P_{0_2}(w, T)$ (or aerobic scope) follows a similar form to the mass budget:

$$P_{0_2}(w, T) = S_{O_2}(w, T) - D_{O_2}(w, T) \tag{4}$$

$$= S_{O_2}c_{O_2}(T)w^n - \omega c(T)\left(\beta f(w, T)hw^q + kw^n + k_a w\right). \tag{5}$$

Demand ($D_{O_2}(w, T)$) is the sum of oxygen used for all metabolic processes in Eq. 2 (except assim-

114 ilation losses), with ω being amount of oxygen required per mass. The oxygen supply ($S_{O_2}c_{O_2}(T)$)

scales with body weight as w^n multiplied by a flexible dome-shaped function that can emulate both

a dome-shaped maximum oxygen supply (MOS) as well as a MOS that increase continuously up

117 to a lethal temperature (fig. 1). The maximum oxygen consumption is the oxygen consumption

during maximal activity level that can be sustained over some time, and is usually termed the

maximum metabolic rate (MMR). Although the MMR is often used synonymously with both max-

120 imum oxygen supply and demand, in some species the maximal oxygen consumption ($D_{O_2}^{max}(T)$) is

not reached at maximum activity levels, but rather during digestion (Priede 1985). We use MMR and oxygen supply interchangeably, although maximum oxygen demand (i.e., at full activity) may be lower than the MMR. We assume that oxygen supply is temperature dependent and follows a flexible dome-shaped function (Gnauck and Straškraba 2013; Lefrancois and Claireaux 2003):

$$s_{O_2}(T) = \lambda(T) \left(1 - e^{(O_2(T) - P_{\text{crit}}) \log(0.5)/(P50 - P_{\text{crit}})}\right), \tag{6}$$

$$\lambda(T) = \zeta \left(\frac{T_{\max} - T}{T_{\max} - T_{\text{opt}}}\right)^{\eta} \times \exp\left(-\eta \frac{T_{\max} - T}{T_{\max} - T_{\text{opt}}}\right), \tag{7}$$

Here $\lambda(T)$ specifies the temperature dependency of O_2 supply, whereas the $s_{O_2}(T)$ term describes the saturation dependence on ambient O_2 at temperature T ($O_2(T)$). At constant temperature T, oxygen supply is a function of ambient oxygen and is assumed to follow a saturating function (e.g., Lefrancois and Claireaux, 2003). We specify P_{50} as the point where oxygen supply has dropped by 50% relative to the saturation level $\lambda(T)$, and P_{crit} is the ambient concentration at which oxygen supply ceases. Ambient oxygen levels are assumed to decline with temperature as $l * \exp(-0.01851 * (T - 5)$, with l the ambient oxygen concentration at 5°C. To specify $\lambda(T)$, we use $T_{\max}$ the lethal temperature for the species, T_{opt} the temperature at which oxygen supply is maximised; η determines the width of the dome-shape, and ζ its height. Note that we can emulate an oxygen supply (and hence maximum metabolic rate; MMR) that increases up to the lethal temperature by setting the temperature for maximum oxygen delivery close to the lethal temperature (fig. 1).

In our model, fish will adjust their activity fraction τ to maximise fitness. We use Gilliam's rule as a fitness proxy Gilliam and Fraser 1987:

$$\tau^* = \text{argmax}_\tau \{\frac{P(w, T)}{M(w)}\}. \tag{8}$$

8

This optimisation represents a "short-sighted" fitness optimisation that does not account for future changes in conditions, and is appropriate for optimisation in stable environments (Sainmont et al. 2015-09). Mortality scales with activity fraction and weight as w^{q-1} (Andersen et al. 2009; Hartvig et al. 2011):

$$M(w) = (\rho + \eta\tau)w^{q-1}, \tag{9}$$

ρ is mortality at mass $w = 1$ and $\tau = 0$, that is, with no activity beyond that covered by standard metabolism. Activity is limited by available oxygen, such that the aerobic scope P_{O_2} is not allowed to be negative over the time scales considered. In other words, we consider time scales that are long enough to ignore the ability of many ectotherms to go into oxygen debt, or to switch to anaerobic metabolism for limited periods of time. This means we assume that animals will adjust their foraging effort to optimise fitness given temperature and oxygen constraints. Note, that this optimal foraging assumption drives ecological responses as a consequence of physiological constraints, rather than as a direct response to temperature itself.

That fish behave optimally to maximise food acquisition relative to mortality risk and energetic requirements is a standard hypothesis and assumption in ecological models (Claireaux et al. 2016-08-08; Gilliam and Fraser 1987; Hufnagl and Peck 2011; Priede 1977; Sainmont et al. 2015-09). Indeed, heightened mortality risk may be a key driver of fish spending very little time in vivo at metabolic regimes that approach the MOS (Priede 1977).

Defining performance metrics

Performance itself is a vague concept that is often used without definition in the relevant literature, but it is only defined in the context of a particular physiological or demographic parameter, with potentially different thermal response curves (Jutfelt et al. 2018). For instance, even though growth

9

in ectotherms is often impacted by temperature (Angilletta et al. 2004), measured performance may depend strongly on what aspect of growth is measured — whether it is the growth increment at a particular size, growth efficiency per unit intake, the attained asymptotic size, or parameters of a fitted growth curve. We use and compare four performance measures with broad ecological and practical implications:

- Growth curves predicted through ontogeny, which allow us to compare growth performance early and late in life (i.e., juvenile growth vs asymptotic size).

- Production efficiency, here defined as available energy for both growth and reproduction, relative to the food consumption (i.e., $\frac{P(w,T)}{f(w,T)hc(T)w^q}$).

- The dimensionless ratio of $\frac{P}{Mw}$, which is analogous to the short-sighted fitness aproximation (Gilliam's rule) used above.

- Fitness integrated over an individual's lifetime, defined as R_0 (see below).

Growth response

Temperature affects growth via its effects on the energy budget and the investment of available (surplus) energy into reproduction and growth. The change in allocation to reproduction with size and age in variable environmental conditions is described by the maturation reaction norm, which is generally defined as the probability of maturing at a certain age under different growth conditions (e.g., Dieckmann and Heino, 2007). We defined the reaction norm as the mid-point of a logistic allocation function that determines investment in reproduction as a function of age and size.

The slope of maturation reaction norms is evolutionarily determined by the strength of the co-variation between growth and mortality for a given population in a given environment. Strongly

10

positive co-variation leads to the relatively flat reaction norms observed for most fish populations (Marty et al. 2011). This covariation is probably the consequence of good growth conditions (e.g.,

183 from increased prey density) altering the baseline mortality ρ and the risk of foraging η (e.g., by attracting predators). We did not explicitly model these interactions here (aside from the dependence of mortality on τ), but rather assumed that reaction norms evolved over regimes of

186 relatively stable temperature and growth variation in the past. Consequently, we assumed that the evolved slope of the reaction norm is a fixed trait over the time-scales considered here for a particular species or population, and for simplicity and generality we assume a flat reaction norm

189 (i.e., allocation to reproduction is a function of size only; fig. A1), although sloping reaction norms can be formulated and used in our framework (see appendix). The intercept of this reaction norm was found numerically by maximising fitness (R_0, see below) at the reference temperature for our

192 simulations (15°C), and this intercept was assumed fixed as temperatures change.

The allocation was parametrised as

$$\phi(w^*) = 1/(1 + \exp(-cw^*))$$

, where w^* is the intercept of the reaction norm, and c determines how rapidly energy allocation

195 shifts from somatic growth to reproduction.

As growth is also fundamentally driven by resource availability, we contrast the growth response to temperature at the baseline level (Table 1), with a 1/3 reduction and increase in available

198 resources.

11

Fitness consequences

Fitness consequences for particular life-history strategies (trait combinations, see below) at different

temperatures can be investigated if one considers the time-scales in the model to be short relative to

evolutionary time-scales (i.e., if the model represents ecological time-scales). On these time-scales,

we assume that adaptive responses are negligible. We investigate over-all fitness with respect to

temperature by calculating R_0 for a given maturation-reaction norm and trait parameters - we thus

do not consider evolutionary consequences of changes in fitness here. R_0 was calculated as

$$R_0(T) = \int_0^\infty \phi(w(t), w^*) P(w(t), T) S_{0 \to t}(T) \mathrm{d}t, \text{ where} \tag{10}$$

$$S_{0 \to t}(T) = \int_0^t \exp(-M(w(t), T)) \mathrm{d}t \tag{11}$$

Trait based scenarios

To ensure a level of generality, we explored ecological impacts of optimised behaviour at different

temperatures in a trait-based context. Specifically, we aimed to contrast species along a gradient

of life-history that, at the one end, maximises production (energy acquisition; henceforth called

the fast strategy, indicated by a subscript f) at the cost of increased metabolism and mortality,

and at the opposing end minimises mortality and metabolic costs at the expense of production

(henceforth slow strategy, indicated by a subscript s). This axis leads to an approximately constant

ratio of production to mortality, and corresponds to a line of equal size in the life-history space

proposed by Charnov et al. (2013). In other words, this axis contrasts species of similar size (here

$L_\infty \sim 30\text{cm}$ or $w_\infty \sim 270\text{g}$) with defensive/sluggish versus active life-histories.

To implement this axis, we used the result that species with a more active, production oriented

life-history (e.g., predatory pelagic fish) have a higher standard metabolism and lower weight scaling of metabolic costs (Killen et al. 2010; Priede 1985). We assumed that higher standard metabolism is due to increased digestive capacity (i.e., is used for gut maintenance), though high muscle mass and a larger heart will also contribute to higher standard metabolism in active species (Priede 1985). In practice, we assumed that approximately 50% of the standard metabolic cost is due to gut maintenance, such that a doubling of the maximum ingestion leads to a 50% increase in standard metabolic cost. We further assumed that such active species have a less effective refuge from predators and therefore have a higher constant mortality, but lower mortality related to activity (i.e., $M_s(w) = (0.1 + 6\tau)w^{q-1}$ and $M_f(w) = (1 + \tau)w^{q-1}$). Exact parameter values for these trait scenarios are given in Table 1. Together, these assumed trait differences lead to very different ecological and bio-energetic responses of slow- and fast strategists (fig. 2), with τ_{opt} found at lower activity levels for slow-strategists, as high activity induces exceedingly high mortality and decreasing energy efficiency (i.e., available energy relative to food intake) at high activity levels. A slower increase in available energy and M with τ for fast strategists leads to a higher τ_{opt}.

We further contrasted species with oxygen limitation at high temperatures (i.e., species with a uni-modal metabolic scope) with species that do not experience oxygen limitation at high temperatures (at least not up to a lethal temperature, where death may be induced by sudden failure to deliver oxygen to vital organs, or failure of bio-chemical pathways at high temperature Iftikar and Hickey 2013; Salin et al. 2016). In practice, this was achieved as described above by setting the maximum oxygen delivery close to the lethal temperature (fig. 1). Note that, although we assume here that limitations over the temperature range are due to oxygen availibility, other limiting mechanisms, such as the respiratory control ratio (Iftikar and Hickey 2013; Salin et al. 2016) may determine upper limits to activity over some or all of a species temperature range. However the

13

over-all mechanism would be the same to the one assumed here, with different untis (e.g., ATP instead of O_2).

Our scenarios were parametrised to allow for excess metabolic scope beyond maximum foraging activity (i.e., $\tau = 1$). This assumption is in line with observations that the aerobic scope often exceeds energetic requirements from swimming alone, and is adapted to provide oxygen for digestion (SDA), the oxygen demand of which can be as high or higher than that of locomotion alone (Priede 1985).

Results

Increasing metabolic demands with temperature lead species to adjust activity levels in order to optimise energy gains relative to mortality risk (fig. 3). This adjustment is especially pronounced in slow strategy species, for which the over-all activity level is markedly lower and which show a consistent increase in activity over-all sizes for the simulated life-history (fig. 4). A similar increase in activity is observed for small fast strategy individuals (e.g., post-larval) for which even initial activity levels are very high (fig. 4). For these individuals, the increasing activity and metabolic demands lead to an active metabolic rate that is close to their MMR. For all other sizes across the two trait scenarios, oxygen is only limiting to activity at the extremes of the simulated temperature range (fig. 3), and only for species with a dome-shaped MOS with respect to temperature. For species with a rising MOS with temperature, oxygen is not limiting (fig. S1). However, larger fast strategy individuals are predicted to show a slightly dome-shaped adjustment in activity levels at intermediate sizes, and a slightly decreasing activity level in response to temperature at large sizes, despite available aerobic scope for activity. This adjsutment is a function of metabolic activity costs assumed here - at smaller metabolic costs per activity, activity adjustment are strictly increasing

14

(fig. S2).

Temperature and metabolic demand-driven adjustments to the activity level lead to substantial changes in performance related metrics in both trait scenarios (fig. 5). For slow strategy species, the increases in activity levels lead to relatively stable feeding levels, but a substantial increase in mortality coupled with a slow increase in available energy leads to an over-all decline in the ratio of P to M. Available energy shows a dome-shaped response to temperature in slow strategists, and is maximised at relatively high temperatures. However, it is limited by oxygen availability only at high temperatures in species with a dome-shaped MOS. Production efficiency follows a near opposite trend due to the relatively flat response in the feeding level f, but temperature driven increases in maximum consumption.

For fast strategists, the relatively modest response in activity levels at all but the smallest sizes leads to a decline in feeding levels, which causes a largely dome-shaped response of available energy and growth efficiency to warmer temperatures (fig. 5). Again, production efficiency peaks at relatively low temperatures, but in this scenario available energy P peaks at much lower temperatures. Given the relatively flat mortality levels, the ratio of P/M largely follows the trend in P.

Simulated growth curves illustrate the ontogenetic consequences of increasing temperatures (fig. 6). For both trait scenarios, fastest growth occurred at relatively high temperatures, with declining growth for oxygen limited species at the highest temperatures (fig. S4). This can be explained by ontogenetic shifts in temperature optima for growth (fig. S3): for small individuals, available energy and growth consistently peak at high temperatures, but this peak rapidly moves to lower temperatures as individuals in either trait-scenario grow. For large individuals, growth is optimised at relatively low temperatures, leading to larger asymptotic size at lower temperatures.

Resource availability strongly modulates this growth response to temperature: low resource

15

availability leads to strong differences in asymptotic size, whereas high food availability leads to fast growth and larger asymptotic length at high temperatures (figs. 6,7). In addition, in very resource poor conditions, individuals may not grow to reproductive size in our scenario of a flat MRN. Over-all growth responses to temperature are not strongly affected by the assumed slope of the MRN (figs. S5,S6), although a negatively sloped MRN does ensure maturation in low resource environments.

Over-all fitness consequences mirror trends in the ratio of P/M (fig. 8a), which can be seen as a short sighted approximation to over-all fitness optimisation (Sainmont et al. 2015-09). With increasing temperatures, fitness declines at our basic parameter settings, in opposition to growth and aerobic scope. At low temperatures, fitness is limited by aerobic scope, with the magnitude determined by the extend of doming in aerobic scope. Note that this limitation through the aerobic scope appears at higher temperatures than apparent from fig. 3, reflecting stronger limitation of oxygen on growth during early life (fig. S3). Fitness trends with temperature are strongly dependent on metabolic costs of activity (fig. 8b), and changing the activity cost to lower values attenuates the decline in fitness with temperature for slow strategy species, and moves the fitness optimum to higher temperatures for fast strategy species. Similarly, increased food availibility leads to changes in fitness optima, with higher optimum temperatures, especially for fast strategists, and a slower decline of fitness with temperature.

Discussion

In this study, we attempt to provide a general mechanistic basis for exploring thermal sensitivities of ectotherm organisms. Much of the recent debate about the validity of projected climate change impact on ectotherms, and fish in particular, has resolved about the validity of particular concepts,

16

such as the OCLTT and projections based on the gill-oxygen limitation theory (Lefevre et al. 2018; Pauly and Cheung 2017). We attempted to go beyond this debate by developing a model that allows for general insights about the temperature response in ectotherms, while being specific enough to mechanistically articulate aspects of physiology and ecology that are fundamental to organism response to temperature. The general model and its parameter values are also easily adjusted to reflect particular organisms or theories.

It has been argued that the OCLTT as a concept provides a basis to explain observed responses to climate change on the basis of oxygen limitation via the aerobic scope (Pörtner 2010; Pörtner and Farrell 2008), and simple oxygen budgets have been used to predict metabolic constraints on organismal activity due to warming ocean temperatures (Deutsch et al. 2015). As a conceptual framework, however, the OCLTT is subject not only to semantic dispute but also criticism of its core concept of oxygen limitation (Jutfelt et al. 2018; Lefevre 2016).

Our quantitative thermal impact model generalises existing eco-physiological models for particular species and stocks (Holt and Jorgensen 2014, 2015; Hufnagl and Peck 2011), and allows to develop a more nuanced understanding of interactions between temperature, oxygen limitation and ecology for species with varying traits. In line with the conceptual framework of Fry's aerobic scope and the OCLTT, our model suggests that oxygen limitation can be a potentially important ecological driver, especially at extreme temperatures for species with declining MOSs in such temperature regimes. At the onset of this limitation, ecological parameters change drastically, and growth, mortality are strongly impacted. This limitation closely mimics limitations seen in wild fish (Myrick and Cech 2000), and is in line with observations that fish often seek specific water temperatures to optimise metabolic function (e.g., Armstrong et al., 2013; Claireaux et al., 1995). Fitness, however, appears to be limited through the metabolic scope primarily via limitations at

17

temperature extremes and impact on particular life-history stages. For instance, oxygen limitation is a more severe constraint for small individuals (fig. S3), and thereby can limit growth performance early in life, impacting over-all fitness. Furthermore, changes in environmental oxygen supply, if beyond an organisms ability to compensate via passive or active compensation mechanisms, will induce an over-all lower aerobic scope and lead to an earlier onset of oxygen limitation, but such scenarios do not change the qualitative predictions from our model.

Variation in performance metrics away from temperature extremes are primarily affected by the interaction of temperature driven metabolic demands with optimal feeding behaviour. Predictions from our model, in line with metabolic experiments and species specific physiological predictions (e.g., Holt and Jorgensen, 2014), suggest that routine activity, including normal swimming behaviour, feeding, and digestion usually lead to routine metabolic rates that are well below the MOS, even in fish with high metabolism (Lucas and Priede 1992; Priede 1985). Strenuous swimming activity, for example, usually only makes up a small proportion of the standard energy budget in fish (Priede 1977, 1985). Furthermore, as a limit for long-term performance, the MOS does not usually impose a limitation on short term energy demands, as fish can incur oxygen debt during swimming bursts during which the MOS is exceeded (Brett 1972; Priede 1985). A logical conclusion is that the metabolic scope is only limiting to performance at extreme temperatures where MOS is low due to impaired oxygen delivery.

In many species, both the aerobic scope and growth peak at relatively high temperatures within the potential thermal range, yet species are often found at temperatures lower than these optima (Claireaux et al. 2016-08-08; Magnuson and DeStasio 1997). Previous explanations of this niche-occupation paradox involved environmental factors that narrow the thermal niche or behaviour that optimises thermal performance across available habitats (Claireaux et al. 2016-08-08; Magnuson

18

and DeStasio 1997). In nearly all our simulation scenarios, fitness is predicted to decline with increasing temperature. This decline with temperature leads to a parsimonious explanation for the relationship between growth performance and fitness at varying temperatures.s

Resource availability imposes a strong environmental constraint on organisms, with all aspects from optimal activity levels, mortality and available energy for growth ultimately influenced by available prey. Changes in prey availability thus influence individual temperature response directly via available energy, and indirectly, through altered energetic requirements to procure food and changes in mortality due to changes in the optimal activity level. In low-food environments, changing energetic demands with temperature are not easily adjusted for, and any adjustment demands higher energetic costs and mortality risk. This environment-driven change in costs of temperature adjustments leads to the strong modulation of the growth response, as well as changing gradients in fitness with temperature in these environments. In particular, in low-food environments, asymptotic size is strongly reduced at high temperatures, whereas this is not necessarily the case in high-food environments. Increased growth and mortality changes in such environments then combine to produce a more strongly domed fitness curve than in environments where food supply is not limiting.

Our model prediction of declining fitness with temperature is particularly sensitive to activity costs, with low activity costs leading to increased fitness at warmer temperatures. Our base-parametrisation is based on the assumption that activity cost k_a reflects the cost of maximal activity (i.e., cost of $\tau = 1$), and has the same pay-off for all life-histories. This approximation may not reflect actual activity cost as swimming at MMR in fast predatory fish is far more efficient than swimming of sluggish fish, such as flatfish (Priede 1985). Such an efficiency gain may occur as a result of more efficient form or physiology, or simply by reduced drag at large size (e.g., whale-

19

sharks), and may be a key requirement to the viability of active pelagic predatory fish in tropical waters.

378   Optimal activity is predicted to increase with temperature in nearly all cases, but it is sensitive to the cost of activity - at higher cost relative to the potential pay-off, activity may even decline at high temeprature. Predictions of increased activity are supported by many observations in

381 experimental and field conditions for both larval and adult fish (Biro et al. 2007; Brown et al. 1989; Claireaux et al. 1995; Sswat et al. 2018). This increase of activity often occurs despite increased mortality (e.g., Biro et al., 2007; Sswat et al., 2018), and serves the necessity to offset increased

384 metabolic expenses. Only large individuals of the simulated fast strategy species will optimally decrease activity as a result of increased temperature. In this case, additional activity will lead to comparatively small gains from feeding relative to the cost of activity and SDA, owing to the

387 non-linearity of the functional response.

Taken together, the physiological processes and optimisation described in our model provide a mechanistic underpinning for observations about changes of ecological rates, such as increasing

390 or dome-shaped consumption or attack-rates with temperature (Biro et al. 2007; Englund et al. 2011; Rall et al. 2012). Depending on the strength of oxygen limitation and the development of the optimal activity level over the range of temperatures considered, attack rates and feeding

393 rates may appear to be steadily increasing via increased optimal activity, or dome-shaped from oxygen limitation or dome-shaped optimal activity. Thus, rather than assuming ad hoc changes in ecological rates in response to temperature that may not be transferable between species and

396 traits, the change in these rates may be mechanistically described in terms of optimal ecological adjustments to physiological constraints.

Similarly, our model provides a mechanistic basis for the temperature-size rule in ectotherms

(Atkinson 1994), without needing to evoke direct changes in ecological rates with temperature. The physiological basis leads to heterogeneous predictions about growth trajectories over ranges of temperature, with various degrees of nesting (i.e., non-crossing) and crossing of growth trajectories possible depending on ecological conditions (e.g., food availability) and physiological traits (figs 6, S4). Due to its reliance on physiological traits and their interaction with ecological variables, our model provides a multi-variate framework to predict heterogeneous temperature impacts on size and growth (Angilletta et al. 2004).

In order to provide a general framework, our model setup is deliberately minimalist, and probably under-parametrised to reflect ecological and life-history aspects of particular species, such as migrations, social behaviour or seasonal energy requirements. As such, this framework provides a null model to assess the diversity of possible responses in fish, and other ectotherms, to temperature in a highly simplified system. Nevertheless, it provides a starting point from which to explore the importance of costs and benefits of particular life-histories and thermal adaptations. For instance, a recent species-specific eco-physiological model for cod (Gadus morhua) that includes similar physiological constraints to our model predicted relatively high fitness at high temperatures (Holt and Jorgensen 2014, 2015). Although this difference is potentially due to the different activity cost coefficients, foraging assumptions and species specific parametrisations in their model, differences may also be due to key assumptions about optimal reproduction: the model of Holt and Jorgensen (2014) assumed that reproductive investment is instantaneously optimised in a changing climate, pointing to the possibility that adaptation of reproductive strategies could offset potential fitness declines with increasing temperatures.

21

Conclusions

The importance of the interaction between ecology, bio-energetics and oxygen limitations in deriving realistic predictions about temperature impacts on ecological rates and fitness calls into question predictions for climate change impacts based on simple models of growth alone (Cheung et al. 2013; Pauly and Cheung 2017). We suggest that the general trait-based approach presented here provides a parsimonious compromise between simplistic approximations that may provide misleading predictions about future ecosystems (Brander et al. 2013; Lefevre et al. 2017), and more complex eco-physiological models such as dynamic energy budget models (e.g., Guiet et al., 2016) and species specific eco-physiology models (Holt and Jorgensen 2014, 2015; Hufnagl and Peck 2011). In addition, our model provides a more explicit, physiology-based mechanistic model to derive general predictions about temperature effects on ectotherms than previous general frameworks such as the OCLTT. Predictions from the OCLTT are both contributing to patterns in fitness and ecological rates shown here, but are also only part of the picture, and we suggest that future improvements of predictive frameworks should center on model critisism and improvements, and leave behind semantic discussions about conceptual constructs that are difficult to explicitly link to data.

Funding

Acknowledgments

The authors would like to thank members of the DTU Centre for Ocean Life modeling group for

₄₄₁ stimulating discussions over the course of the development of the ideas in this paper.

Appendix A: Maturation-reaction norm

A flat maturation reaction norm (MRN) leads to a logistic allocation to reproduction that is only

444   dependent on size and independent of age (fig. A1).

To express a MRN that varies as a function of age, we can reparametrise the MRN as:

$$\phi(z) = 1/(1 + \exp(-(cz))), \text{ where} \tag{12}$$

$$z(t, w_t) = (w_t - w^*) \times \cos(\mathrm{atan}(b)) - t \times \sin(\mathrm{atan}(b)) \tag{13}$$

rotates the coordinate system about the slope b of the reaction norm, t is the age, w is the

mass, w^* is the intercept of the reaction norm, and c determines how rapidly energy allocation

447   shifts from somatic growth to reproduction.

References

Andersen, K. H., K. D. Farnsworth, M. Pedersen, H. Gislason, and J. E. Beyer. 2009. How community ecology links natural mortality, growth, and production of fish populations. ICES Journal of Marine Science: Journal du Conseil 66:1978–1984.

Angilletta, M. J., T. D. Steury, and M. W. Sears. 2004. Temperature, growth rate, and body size in ectotherms: Fitting pieces of a life-history puzzle. Integrative and Comparative Biology 44:498–509.

Armstrong, J. B., D. E. Schindler, C. P. Ruff, G. T. Brooks, K. E. Bentley, and C. E. Torgersen. 2013. Diel horizontal migration in streams: juvenile fish exploit spatial heterogeneity in thermal and trophic resources. Ecology 94:2066–2075.

Atkinson, D. 1994. Temperature and organism size: a biological law for ectotherms? Advances in ecological research 25:1–1.

Biro, P. A., J. R. Post, and D. J. Booth. 2007. Mechanisms for climate-induced mortality of fish populations in whole-lake experiments. Proceedings of the National Academy of Sciences 104:9715–9719.

Brander, K., A. Neuheimer, K. H. Andersen, and M. Hartvig. 2013. Overconfidence in model projections. ICES Journal of Marine Science 70:1065–1068.

Brett, J. 1965. The relation of size to rate of oxygen consumption and sustained swimming speed of sockeye salmon (oncorhynchus nerka). Journal of the Fisheries Board of Canada 22:1491–1501.

Brett, J. R. 1972. The metabolic demand for oxygen in fish, particularly salmonids, and a comparison with other vertebrates. Respiration physiology 14:151–170.

Brown, J. A., P. Pepin, D. A. Methven, and D. C. Somerton. 1989. The feeding, growth and behaviour of juvenile cod, gadus morhua l., in cold environments. Journal of Fish Biology 35:373–380.

Brown, J. H., J. F. Gillooly, A. P. Allen, V. M. Savage, and G. B. West. 2004. Toward a metabolic theory of ecology. Ecology 85:1771–1789.

Charnov, E. L., H. Gislason, and J. G. Pope. 2013. Evolutionary assembly rules for fish life histories. Fish and Fisheries 14:213–224.

Cheung, W. W., J. L. Sarmiento, J. Dunne, T. L. Frölicher, V. W. Lam, M. D. Palomares, R. Watson, and D. Pauly. 2013. Shrinking of fishes exacerbates impacts of global ocean changes on marine ecosystems. Nature Climate Change 3:254–258.

Claireaux, G., and C. Lefrançois. 2007. Linking environmental variability and fish performance: integration through the concept of scope for activity. Philosophical Transactions of the Royal Society B: Biological Sciences 362:2031–2041.

Claireaux, G., D. Webber, S. Kerr, and R. Boutilier. 1995. Physiology and behaviour of free-swimming atlantic cod (gadus morhua) facing fluctuating temperature conditions. Journal of Experimental Biology 198:49–60.

Claireaux, G., D. M. Webber, J.-P. Lagardère, and S. R. Kerr. 2016-08-08. Influence of water temperature and oxygenation on the aerobic metabolic scope of atlantic cod (gadus morhua). Journal of Sea Research 44:257–265.

26

Deutsch, C., A. Ferrel, B. Seibel, H.-O. Pörtner, and R. B. Huey. 2015. Climate change tightens a metabolic constraint on marine habitats. Science 348:1132–1135.

Dieckmann, U., and M. Heino. 2007. Probabilistic maturation reaction norms: their history, strengths, and limitations. Marine Ecology Progress Series 335:253–269.

Englund, G., G. Öhlund, C. L. Hein, and S. Diehl. 2011. Temperature dependence of the functional response. Ecology Letters 14:914–921.

Fry. 1947. Effects of the environment on animal activity .

Gilliam, J. F., and D. F. Fraser. 1987. Habitat selection under predation hazard: test of a model with foraging minnows. Ecology 68:1856–1862.

Glazier, D. S. 2009. Activity affects intraspecific body-size scaling of metabolic rate in ectothermic animals. Journal of Comparative Physiology B 179:821–828.

Gnauck, A., and M. Straškraba. 2013. Freshwater ecosystems: modelling and simulation, vol. 8. Elsevier.

Guiet, J., O. Aumont, J.-C. Poggiale, and O. Maury. 2016. Effects of lower trophic level biomass and water temperature on fish communities: A modelling study. Progress in Oceanography 146:22–37.

Hartvig, M., K. H. Andersen, and J. E. Beyer. 2011. Food web framework for size-structured populations. Journal of Theoretical Biology 272:113–122.

Holt, R. E., and C. Jorgensen. 2014. Climate warming causes life-history evolution in a model for atlantic cod (gadus morhua). Conservation Physiology 2.

27

Holt, R. E., and C. Jorgensen. 2015. Climate change in fish: effects of respiratory constraints on optimal life history and behaviour. Biology Letters 11:20141032–20141032.

Hufnagl, M., and M. A. Peck. 2011. Physiological individual-based modelling of larval atlantic herring (clupea harengus) foraging and growth: insights on climate-driven life-history scheduling. ICES Journal of Marine Science 68:1170–1188.

Iftikar, F. I., and A. J. R. Hickey. 2013. Do mitochondria limit hot fish hearts? understanding the role of mitochondrial function with heat stress in notolabrus celidotus. PLOS ONE 8:e64120.

Jeschke, J. M., M. Kopp, and R. Tollrian. 2002. Predator functional responses: discriminating between handling and digesting prey. Ecological Monographs 72:95–112.

Jutfelt, F., T. Norin, R. Ern, J. Overgaard, T. Wang, D. J. McKenzie, S. Lefevre, G. E. Nilsson, N. B. Metcalfe, and A. J. Hickey. 2018. Oxygen-and capacity-limited thermal tolerance: blurring ecology and physiology. Journal of Experimental Biology 221:jeb169615.

Killen, S. S., D. Atkinson, and D. S. Glazier. 2010. The intraspecific scaling of metabolic rate with body mass in fishes depends on lifestyle and temperature. Ecology Letters 13:184–193.

Lefevre, S. 2016. Are global warming and ocean acidification conspiring against marine ectotherms? a meta-analysis of the respiratory effects of elevated temperature, high CO2 and their interaction. Conservation Physiology 4.

Lefevre, S., D. J. McKenzie, and G. E. Nilsson. 2017. Models projecting the fate of fish populations under climate change need to be based on valid physiological mechanisms. Global Change Biology .

Lefevre, S., D. J. McKenzie, and G. E. Nilsson. 2018. In modelling effects of global warming, invalid assumptions lead to unrealistic projections. Global change biology 24:553–556.

Lefrancois, C., and G. Claireaux. 2003. Influence of ambient oxygenation and temperature on metabolic scope and scope for heart rate in the common sole solea solea. Marine Ecology Progress Series 259:273–284.

Lucas, M. C., and I. G. Priede. 1992. Utilization of metabolic scope in relation to feeding and activity by individual and grouped zebrafish, brachydanio rerio (hamilton-buchanan). Journal of Fish Biology 41:175–190.

Magnuson, J. J., and B. T. DeStasio. 1997. Thermal niche of fishes and global warming. Pages 377–408 in C. Wood and D. McDonald, eds. Global warming: implications for freshwater and marine fish, vol. 61. Cambridge University Press.

Marty, L., U. Dieckmann, M.-J. Rochet, and B. Ernande. 2011. Impact of environmental covariation in growth and mortality on evolving maturation reaction norms. The American Naturalist 177:E98–E118.

Myrick, C. A., and J. J. Cech. 2000. Temperature influences on california rainbow trout physiological performance. Fish Physiology and Biochemistry 22:245–254.

Parmesan, C., and G. Yohe. 2003. A globally coherent fingerprint of climate change impacts across natural systems. Nature 421:37–42.

Pauly, D., and W. W. L. Cheung. 2017. Sound physiological knowledge and principles in modeling shrinking of fishes under climate change. Global Change Biology 24:e15–e26.

Pinsky, M. L., B. Worm, M. J. Fogarty, J. L. Sarmiento, and S. A. Levin. 2013. Marine taxa track local climate velocities. Science 341:1239–1242.

Priede, I. G. 1977. Natural selection for energetic efficiency and the relationship between activity level and mortality. Nature 267:610–611.

———. 1985. Metabolic scope in fishes. Pages 33–64 in Fish Energetics. Springer.

Pörtner, H.-O. 2010. Oxygen-and capacity-limitation of thermal tolerance: a matrix for integrating climate-related stressor effects in marine ecosystems. The Journal of experimental biology 213:881–893.

Pörtner, H. O., and A. P. Farrell. 2008. Physiology and climate change. Science 322:690–692.

Rall, B. C., U. Brose, M. Hartvig, G. Kalinkat, F. Schwarzmüller, O. Vucic-Pestic, and O. L. Petchey. 2012. Universal temperature and body-mass scaling of feeding rates. Phil. Trans. R. Soc. B 367:2923–2934.

Sainmont, J., K. H. Andersen, U. H. Thygesen, O. Fiksen, and A. W. Visser. 2015-09. An effective algorithm for approximating adaptive behavior in seasonal environments. Ecological Modelling 311:20–30.

Salin, K., S. K. Auer, G. J. Anderson, C. Selman, and N. B. Metcalfe. 2016. Inadequate food intake at high temperatures is related to depressed mitochondrial respiratory capacity. Journal of Experimental Biology 219:1356–1362.

Sentis, A., J.-L. Hemptinne, and J. Brodeur. 2013. Parsing handling time into its components: implications for responses to a temperature gradient. Ecology 94:1675–1680.

Sswat, M., M. H. Stiasny, F. Jutfelt, U. Riebesell, and C. Clemmesen. 2018. Growth performance and survival of larval atlantic herring, under the combined effects of elevated temperatures and CO2. PLOS ONE 13:e0191947.

Stuart-Smith, R. D., G. J. Edgar, N. S. Barrett, S. J. Kininmonth, and A. E. Bates. 2015. Thermal biases and vulnerability to warming in the world's marine fauna. Nature 528:88–92.

Verberk, W. C. E. P., J. Overgaard, R. Ern, M. Bayley, T. Wang, L. Boardman, and J. S. Terblanche. 2016. Does oxygen limit thermal tolerance in arthropods? a critical review of current evidence. Comparative Biochemistry and Physiology Part A: Molecular & Integrative Physiology 192:64–78.

Vucic-Pestic, O., R. B. Ehnes, B. C. Rall, and U. Brose. 2011. Warming up the system: higher predator feeding rates but lower energetic efficiencies. Global Change Biology 17:1301–1310.

Walther, G.-R., E. Post, P. Convey, A. Menzel, C. Parmesan, T. J. C. Beebee, J.-M. Fromentin, O. Hoegh-Guldberg, and F. Bairlein. 2002. Ecological responses to recent climate change. Nature 416:389–395.

Table 1: Parameters of the constrained activity model for two scenarios: slow strategy and fast strategy species. For parameters with dual values (i.e., x/y), the former reflects species with a domed maximum oxygen supply (MOS) with respect to temperature, whereas the latter corresponds to species with a continuously increasing MOS. Values in brackets for γ are alternative resource availability scenarios.

Description	Symbol (unit)	Value slow strategy	fast strategy
Biomass Metabolism			
Specific dynamic action	β	0.15	
Egestion and excretion	ϕ	0.25	
Coeff. for std. metabolism	k (g^{1-n}·y^{-1})	1	1.5
Coeff. for act. metabolism	k (g·y^{-1})	4	2
Exponent for std. metabolism	n	0.88	0.75
Feeding ecology			
Coeff. for Encountered food	$\gamma\Theta$ (g^{1-p}·y^{-1})	60 (40/80)	
Exponent for clearance rate γ	p	0.8	
Coeff. for Maximum consumption rate	h (g^{1-q}·y^{-1})	30	60
Exponent for max. consumption h	q	0.8	
Coeff. for constant mortality	M (g·y^{-1})	0.1	1
Coeff. for activity related mortality	ρ(y^{-1})	6	1
Exponent for mortality	ν	0.2	
Temperature			
Reference temperature	T_{ref} (°C)	15	
Activation energy	E_a	0.52	
Temperature at maximum MOS	T_{max}	20/25	
Temperature range	T_{lethal}^{-}–T_{lethal}^{+}	5–26	
Reaction norm			
Slope		0	
Reaction	c	0.5	
Oxygen budget			
Critical O_2	P_{crit} (mg·L^{-1})	33	2
Dissolved O_2 at $0.5 \times f_{\mathrm{max}}(O_2)$	P_{50} (mg·L^{-1})	4	
Doming for O_2 supply	η	3/0.1	
Level of O_2 supply	ζ (g·y^{-1})	0.5	1
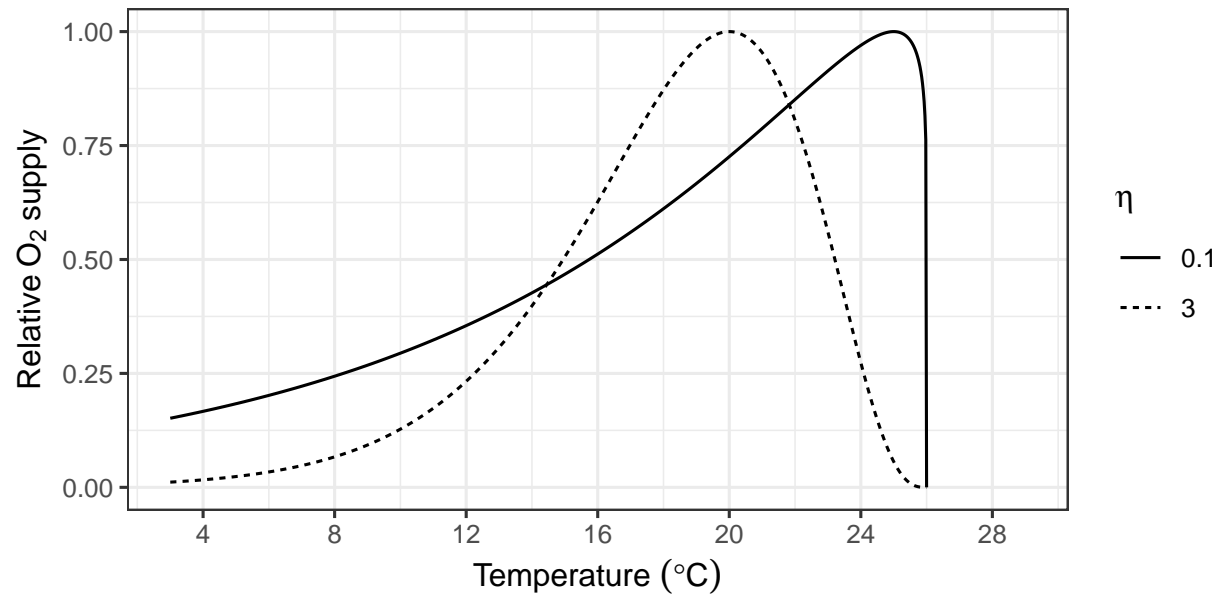
Figures

Figure 1: Maximum oxygen supply relative to the maximum supply for species with a dome-shaped MOS (here $\eta = 3$) and a continually increasing MOS ($\eta = 0.1$) used in model scenarios discussed below.
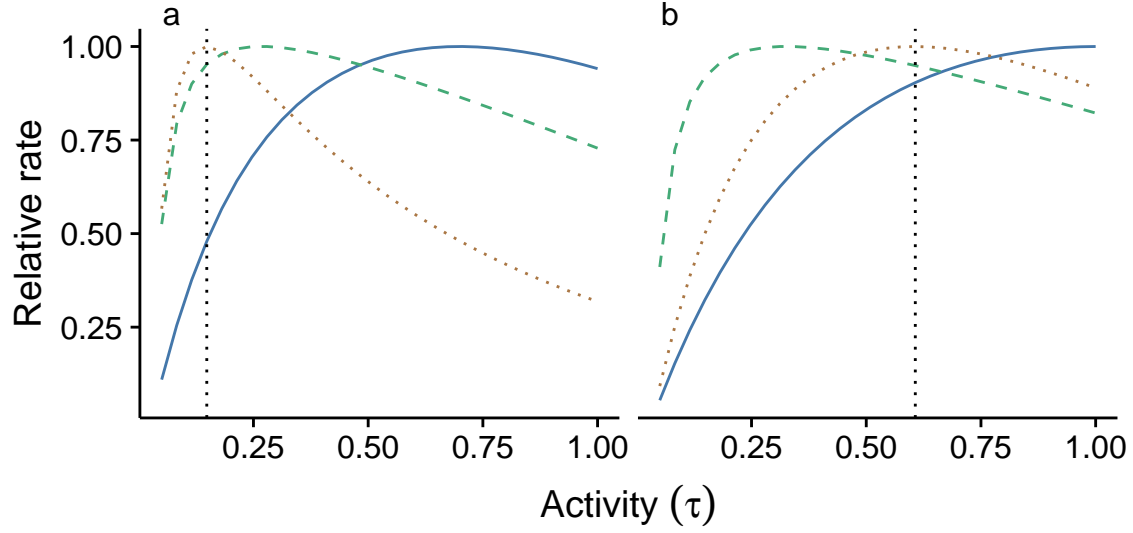
Figure 2: Available energy P (Blue solid line), efficiency (green dashed line), and the ratio of P to M (orange dotted line) are impacted as a function of changing activity at constant temperature $(T = 15°C)$ for a growing fish $(L_\infty \sim 30cm)$ at 10cm length (10g). Responses are shown for slow-(a) and fast strategy (b). All rates are plotted relative to their maximum for each trait scenario, the optimal activity level τ^* is indicated by the dotted vertical line.
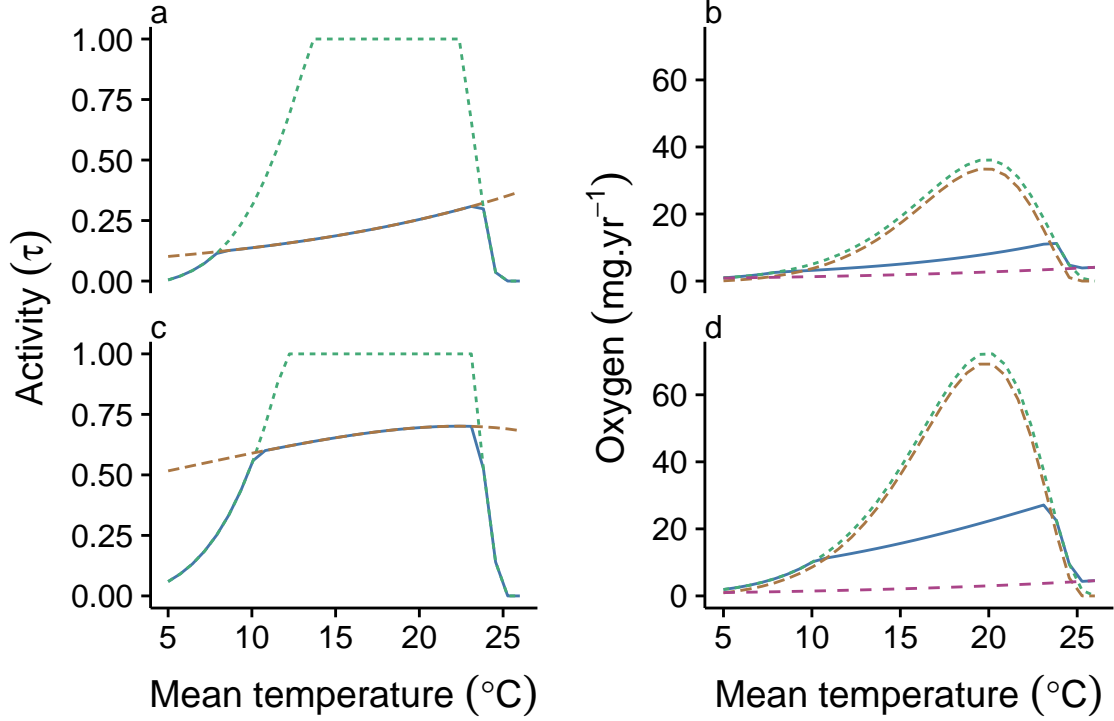
Figure 3: Optimum (red long-dashed), maximum (green short-dashed) and realised (blue solid lines) activity levels (left column [a,c]) at increasing temperatures for a 10g fish with a dome-shaped MOS with increasing temperature (maximum at 20°C), with corresponding oxygen demand (right column [b,d]); maximum oxygen supply (MOS; green short-dashed), standard metabolism (red long-dashed) and realised (active; blue solid lines) metabolic demand, as well as metabolic scope (orange long-dashed) at activity level τ, for slow strategy (slow life history; a & b) and fast strategy (fast life-history; c & d).
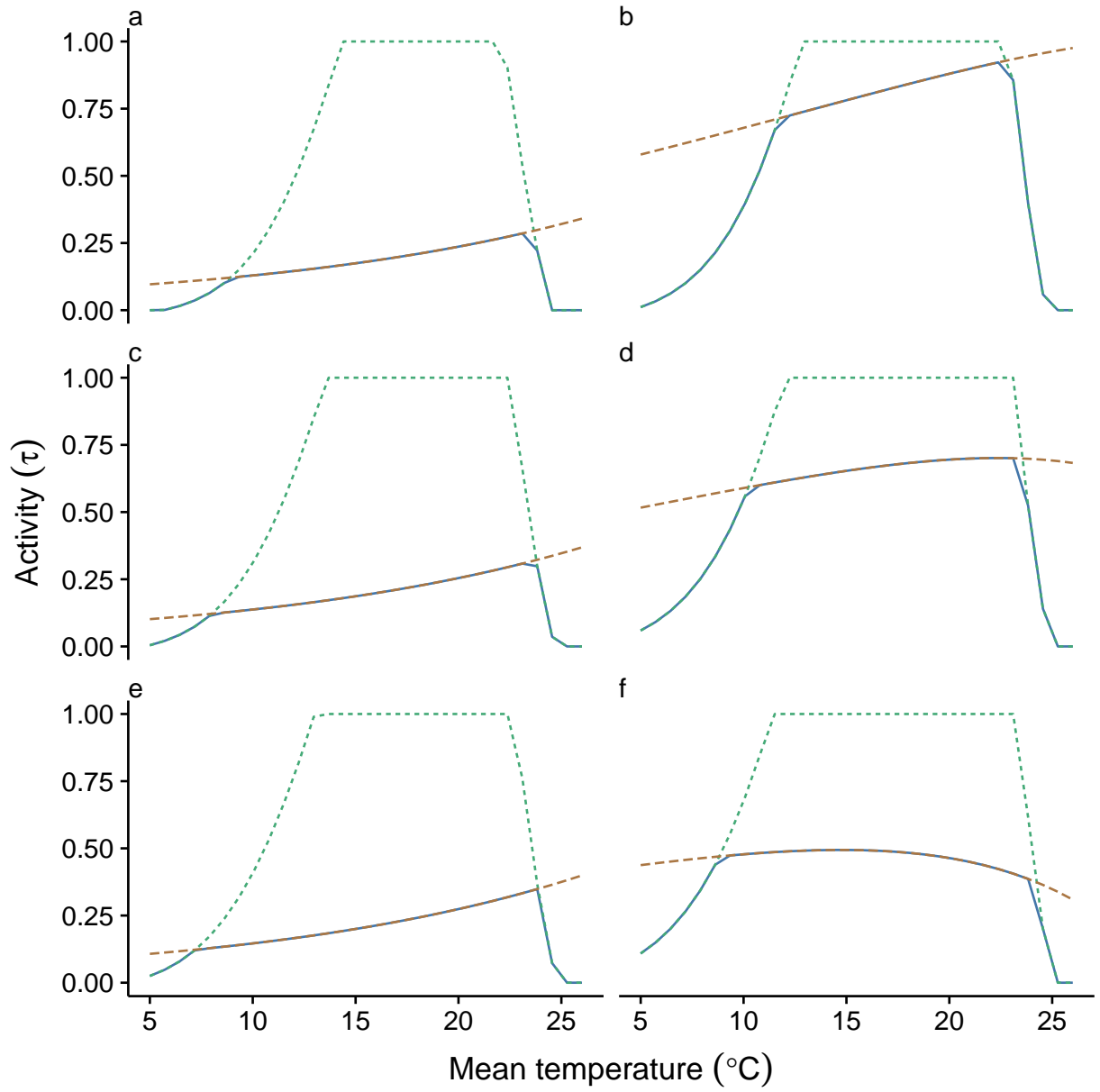
Figure 4: Optimum (red long-dashed), maximum (green short-dashed) and realised (blue solid lines) activity levels (left column) at increasing temperatures through ontogeny for a for fish with a $L_\infty \sim 30$cm at 1.25g (5cm; a–b); 10g (10cm; c–d) and 80g (20cm; e–f), for slow strategy (slow life history; left column [a,c,e]) and fast strategy (fast life-history; right column [b,d,f]) species with a dome-shaped maximum metabolic rate with respect to temperature.
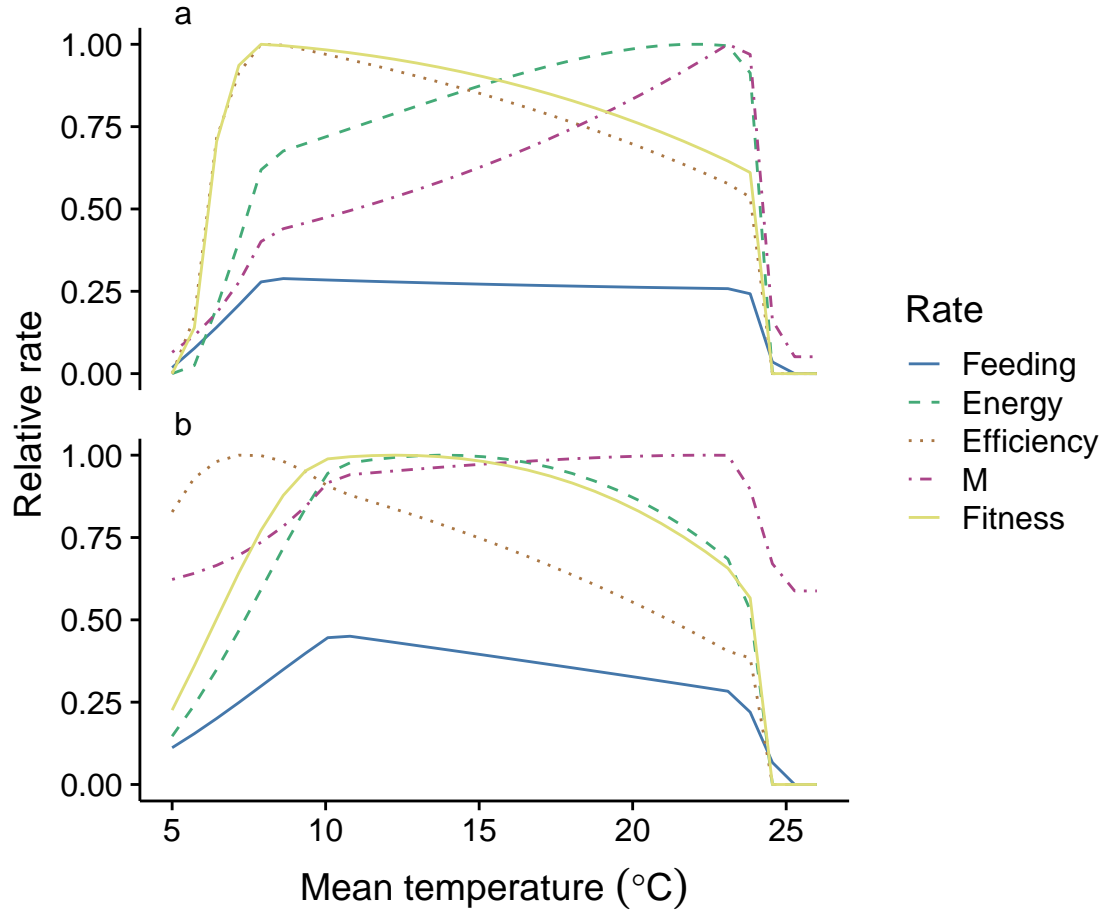
Figure 5: Feeding level (blue solid line), available energy P (green long-dashed), efficiency (orange dotted), mortality (red dotted-dashed) and the ratio of P to M (yellow solid) are impacted by changing activity and the metabolic response to temperature for a growing fish ($L_\infty \sim 30$cm) at 10cm length (10g). Responses are shown for slow and fast strategy (a and b, respectively), for species with and without oxygen limitation (left and right columns, respectively). Energy, mortality and fitness are plotted relative to their maximum over all temperatures.
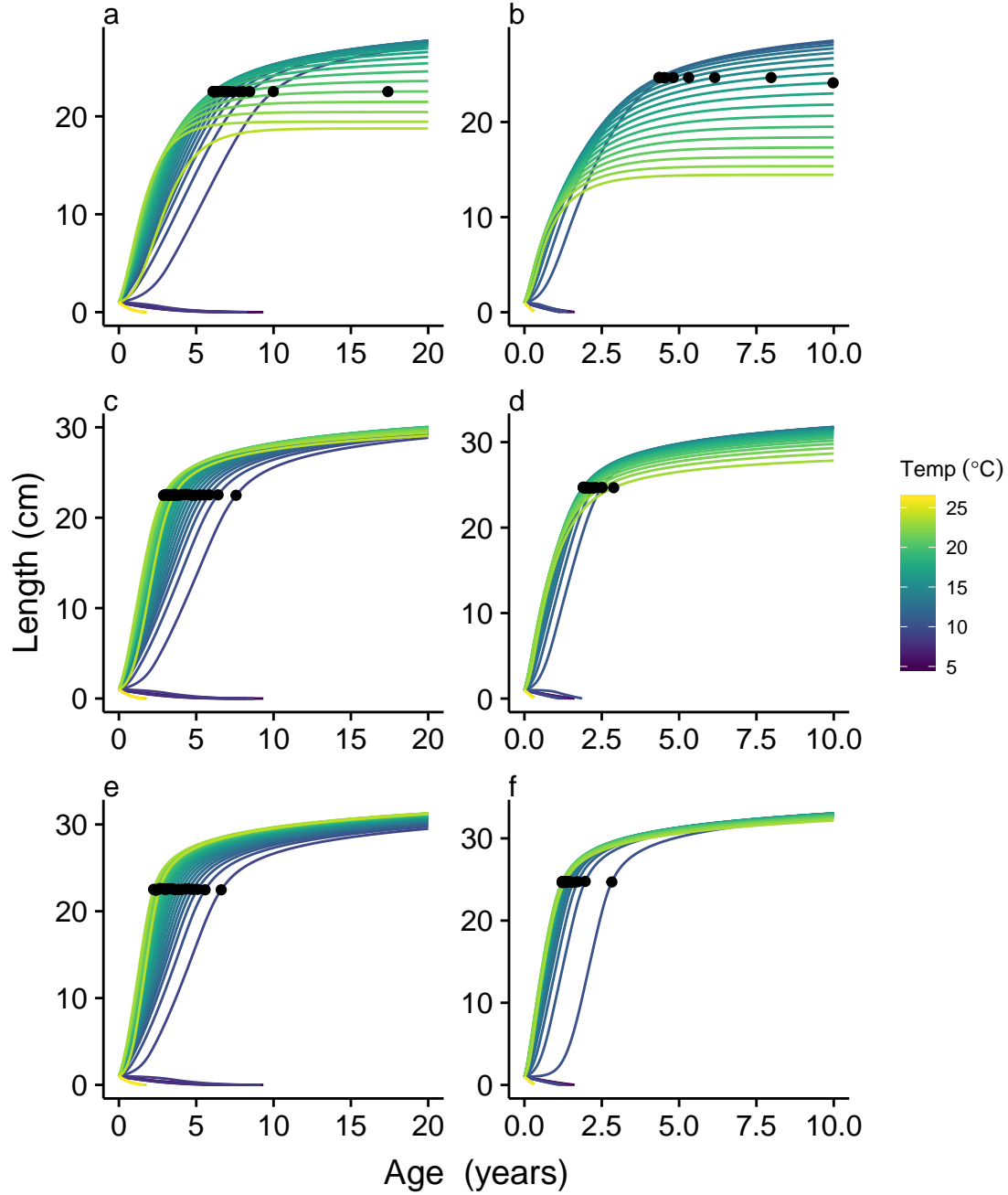
Figure 6: On ecological time-scales, increasing temperature (purple to yellow growth curves) modifies growth, and maturation age changes according to the reaction norm (black dots at 50% allocation to reproduction), whereas asymptotic size is affected by changes in absolute energy available for growth. Growth curves are shown for slow- (left column [a,c,e]) and fast strategists (right column [b,d,f]), at increasing food availibility from top (a/b) to bottom (e/f). Baseline resource availibility assumed in all other simulations is that shown in panels c and d.
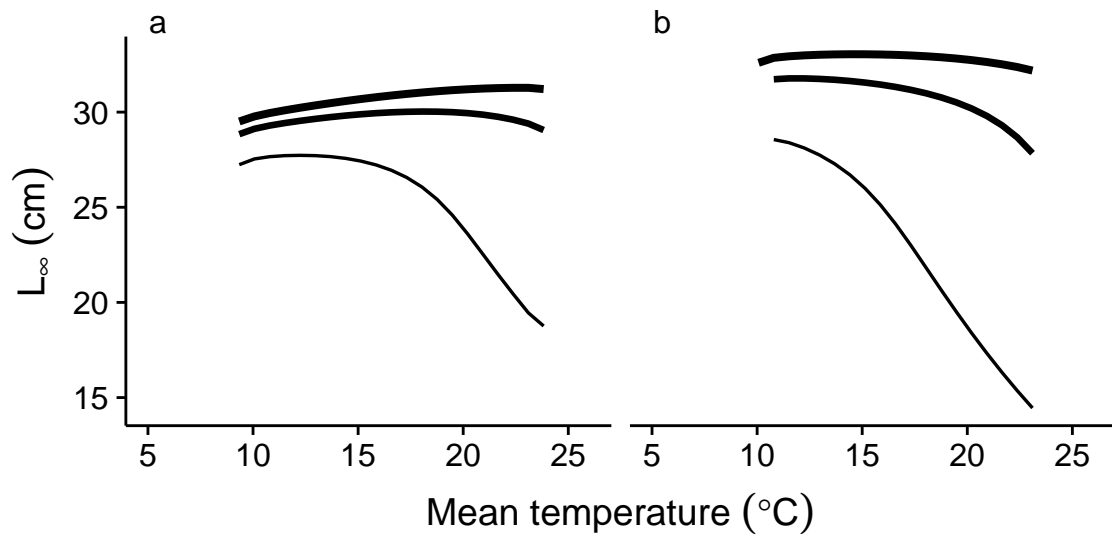
Figure 7: Interactive effects of food availibility and temperature of the asymptotic size (L_∞), with increasing linewidth showing increasing prey availibility for a) slow and b) fast life-history species.
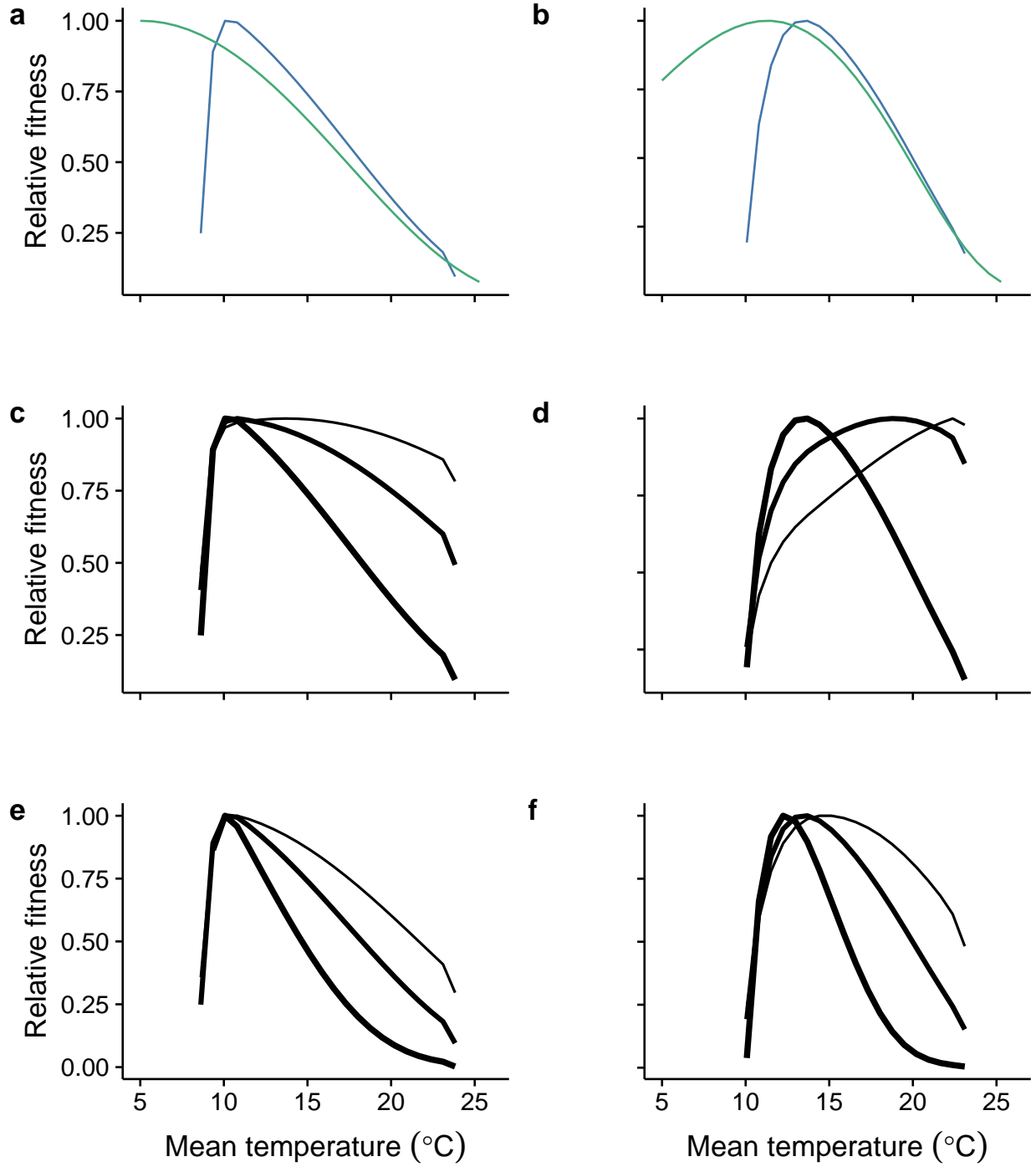
Figure 8: Fitness (R_0), relative to maximum fitness within (a and b) oxygen limited (blue) and non-oxygen limited (teal) for slow- (a) and fast strategy (b) species at the assumed maturation-raction norm and base parameters, and (c and d) changes in relative fitness with respect to temperature resulting from decreasing levels of activity cost symbolised by decreasing linewidth, and (e and f) changes in relative fitness with respect to temperature as a function of increasing food availability

Supplementary Figures
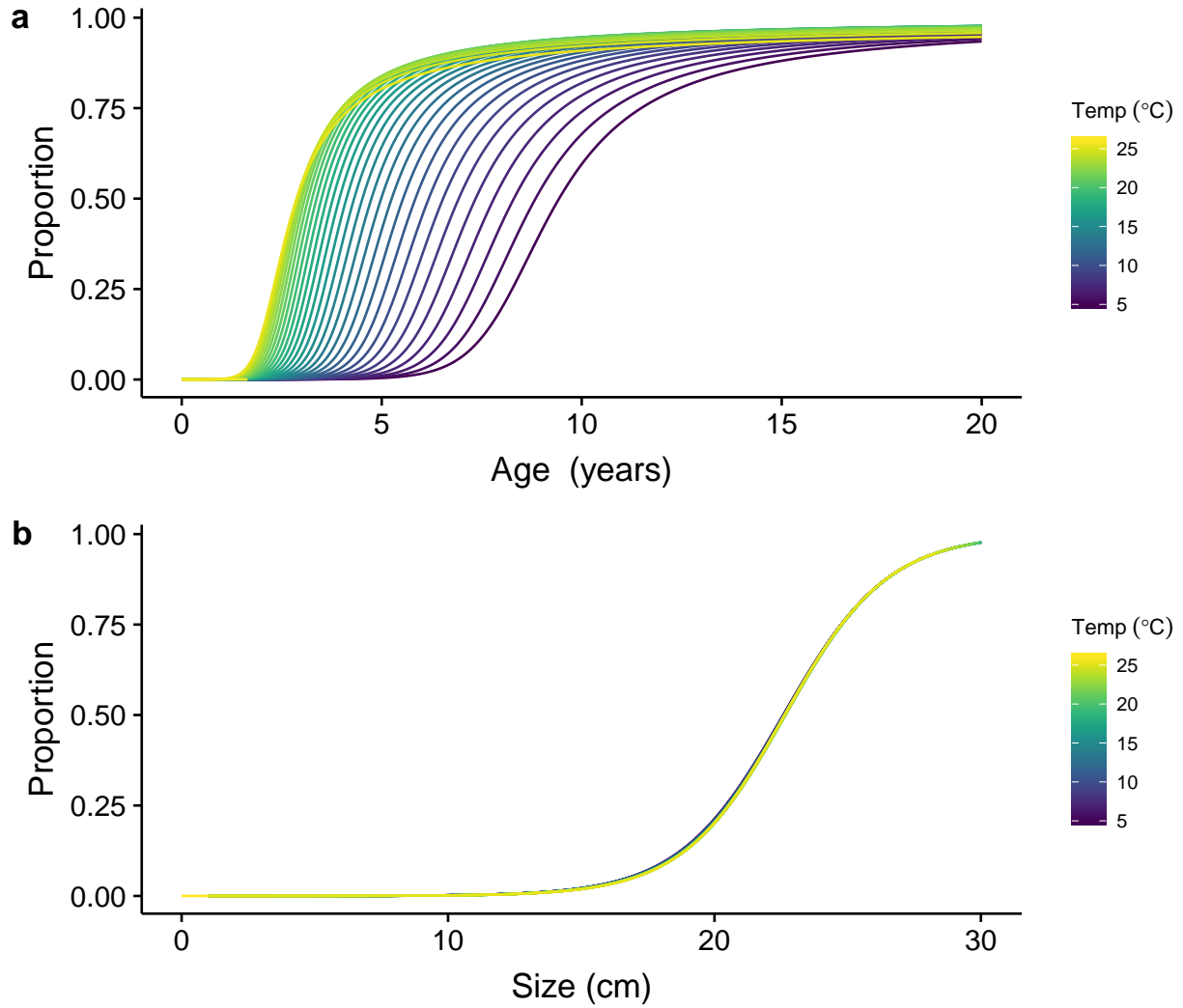
Figure A1: Proportion of energy allocated to reproduction, as a function of age (a) and size (b).

With a flat maturation-reaction norm, maturation is independent of age, and only size-dependent.
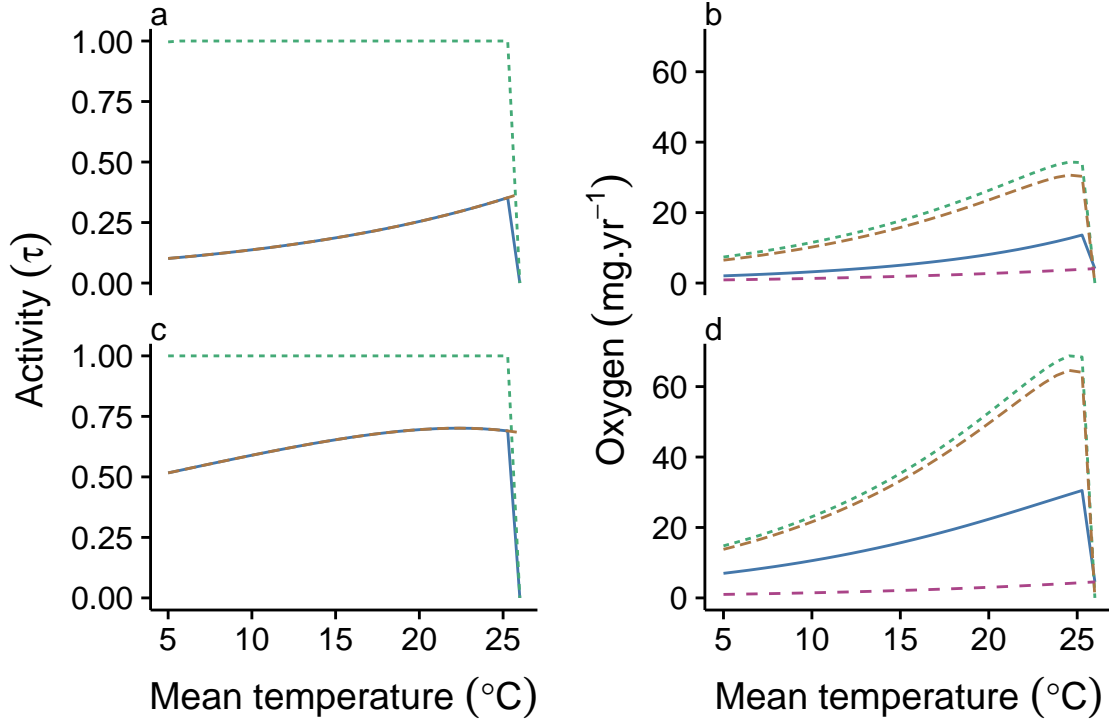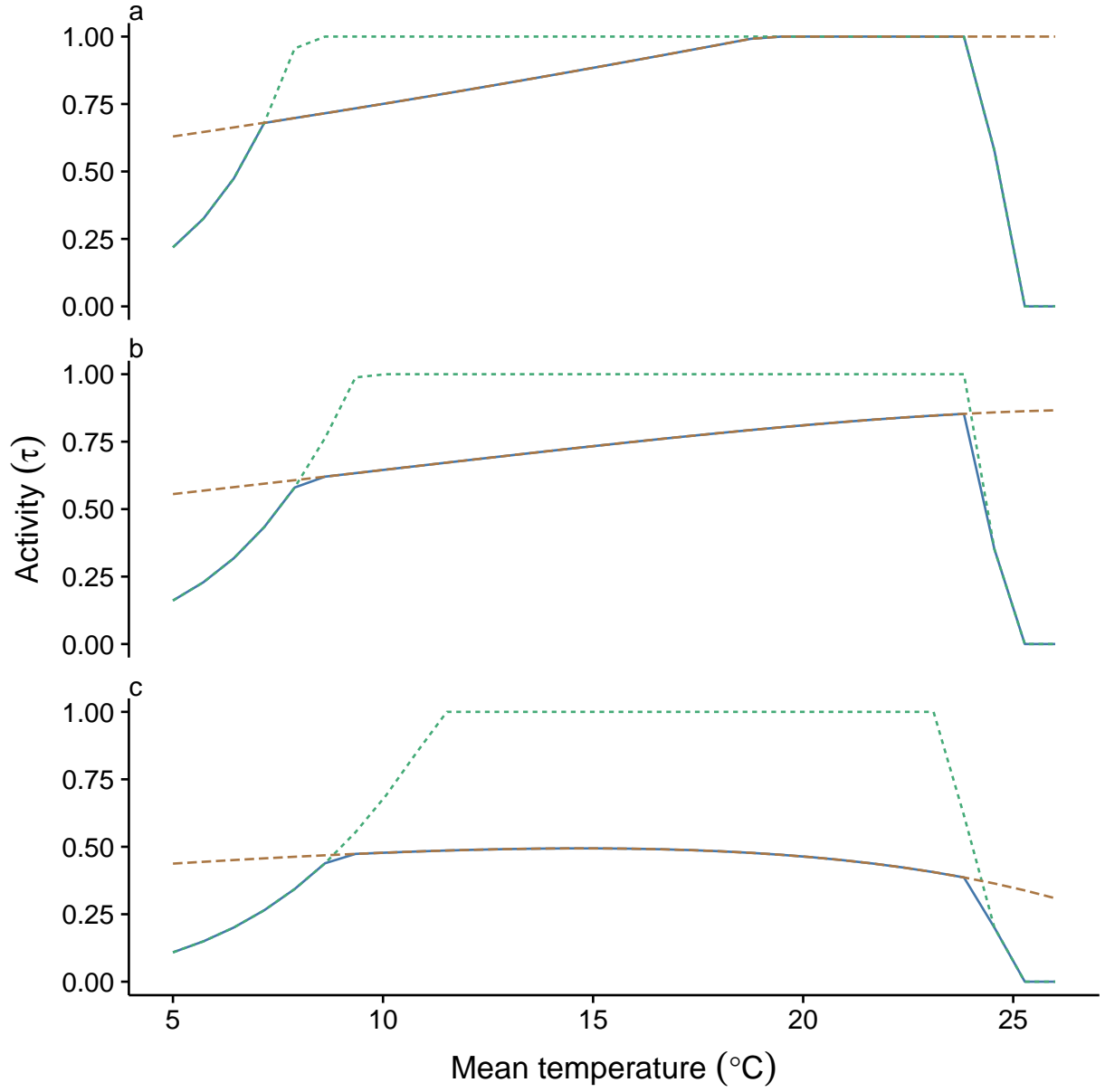
Figure S1: Optimum (red long-dashed), maximum (green short-dashed) and realised (blue solid lines) activity levels (left column [a,c]) at increasing temperatures for a 10g fish with a continuously increasing MOS with increasing temperature, with corresponding oxygen demand (right column [b,d]); maximum oxygen supply (MOS; green short-dashed), standard metabolism (red long-dashed) and realised (active; blue solid lines) metabolic demand, as well as metabolic scope (orange long-dashed) at activity level τ, for slow strategy (slow life history; aandb) and fast strategy (fast life-history; c, d).

Figure S2: Optimum (red long-dashed), maximum (green short-dashed) and realised (blue solid lines) activity levels at increasing temperatures through ontogeny for a for fish nearly grown fish of 80g (20cm; e–f), for a fast strategy (fast life-history) species with a dome-shaped maximum metabolic rate with respect to temperature.
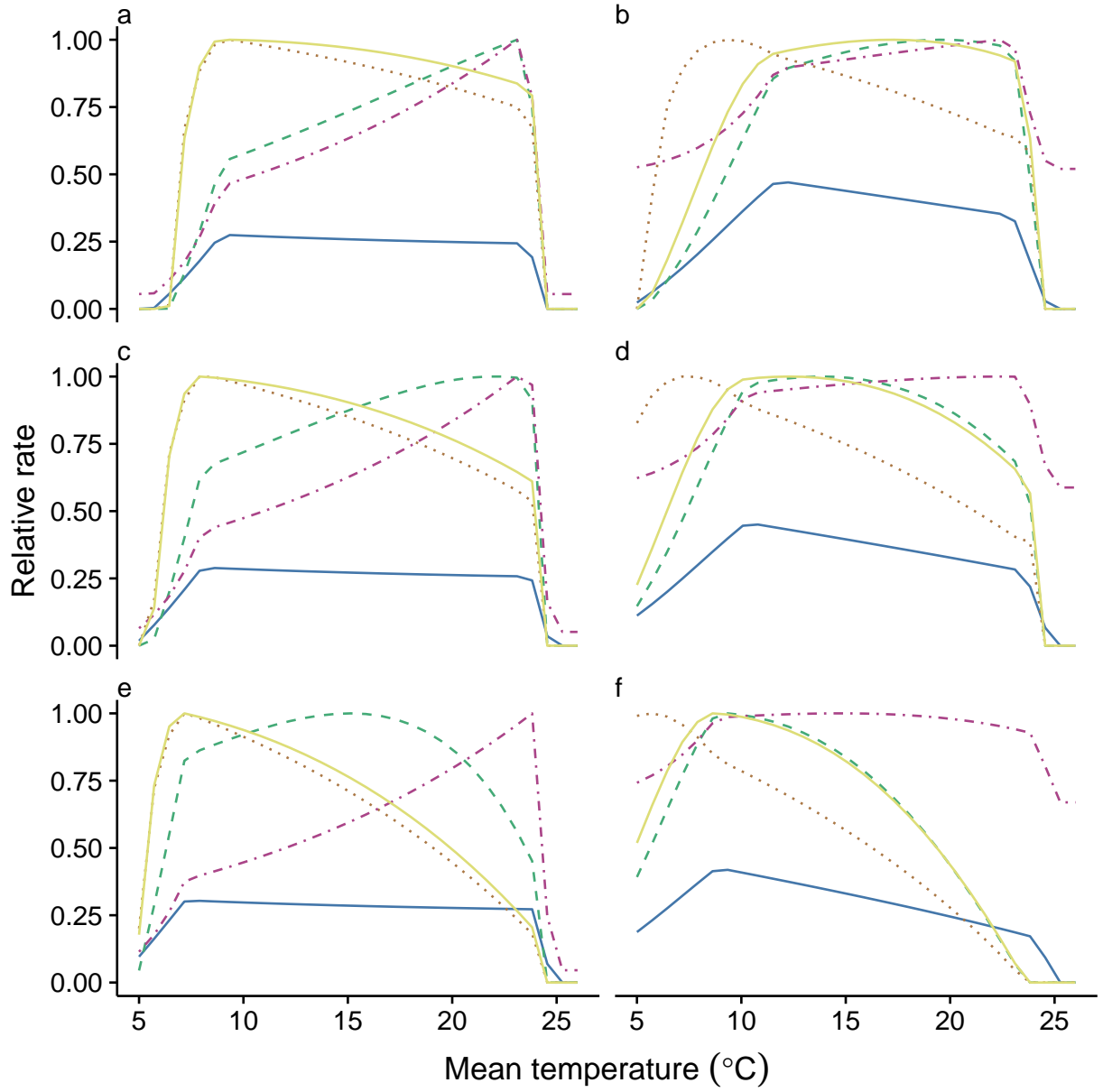
Figure S3: Feeding level (blue solid line), available energy P (green long-dashed), efficiency (orange dotted), mortality (red dotted-dashed) and the ratio of P to M (yellow solid) are impacted by changing activity and the metabolic response to temperature for growing fish ($L_\infty \sim 30$cm) of 1.25g (5cm; a–b); 10g (10cm; c–d) and 80g (20cm; e–f), for slow strategy (slow life history; left column [a,c,e]) and fast strategy (fast life-history; right column [b,d,f]) species with a dome-shaped maximum metabolic rate with respect to temperature. Energy, mortality and fitness are plotted relative to their maximum over all temperatures.
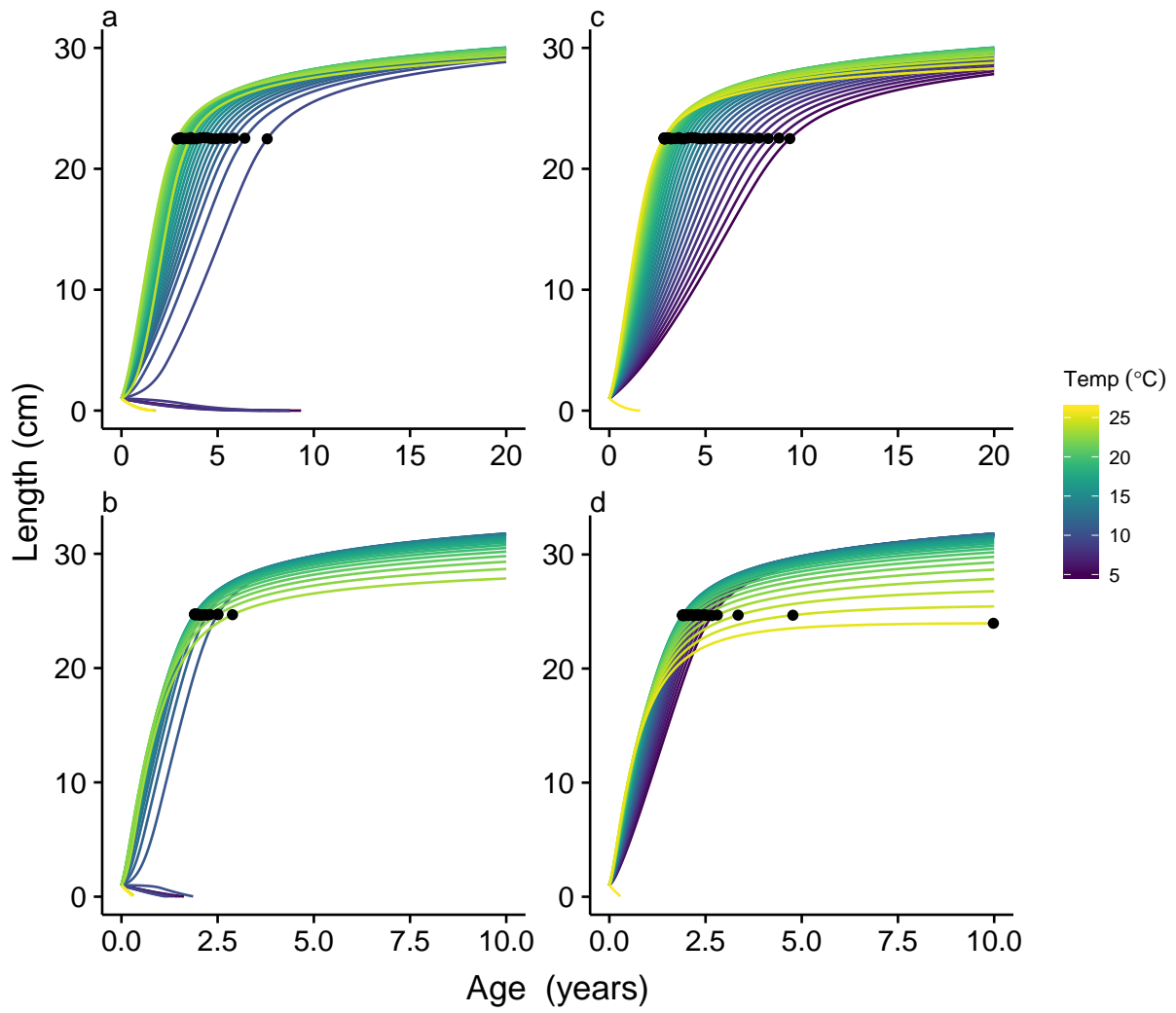
Figure S4: Contrasting growth responses at baseline resource availability for species with dome-shaped MOS (top row [a,b]) and increasing MOS with temperature (bottom row [c,d]). Growth curves are shown for slow- (left column [a,c]) and fast strategists (right column [b,d]). Increasing temperature (purple to yellow growth curves) modifies growth, and maturation age changes according to the reaction norm (black dots at 50% allocation to reproduction), whereas asymptotic size is affected by changes in absolute energy available for growth.
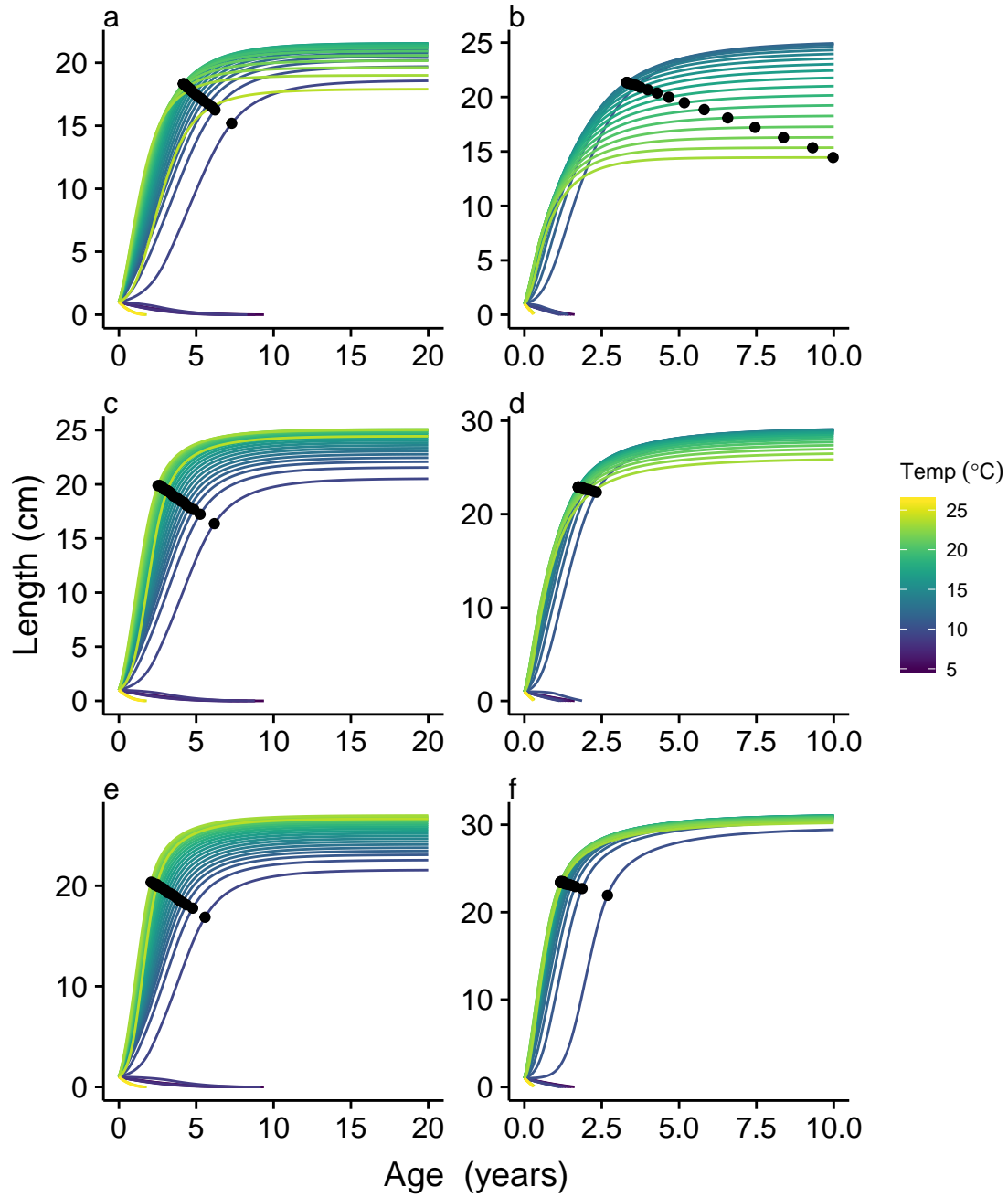
Figure S5: On ecological time-scales, increasing temperature (purple to yellow growth curves) modifies growth, and maturation age changes according to the negative reaction norm (black dots at 50% allocation to reproduction), whereas asymptotic size is affected by changes in absolute energy available for growth. Growth curves are shown for slow- (left column [a,c,e]) and fast strategists (right column [b,d,f]), at increasing food availibility from top (a/b) to bottom (e/f). Baseline resource availibility assumed in all other simulations is that shown in panels c and d.
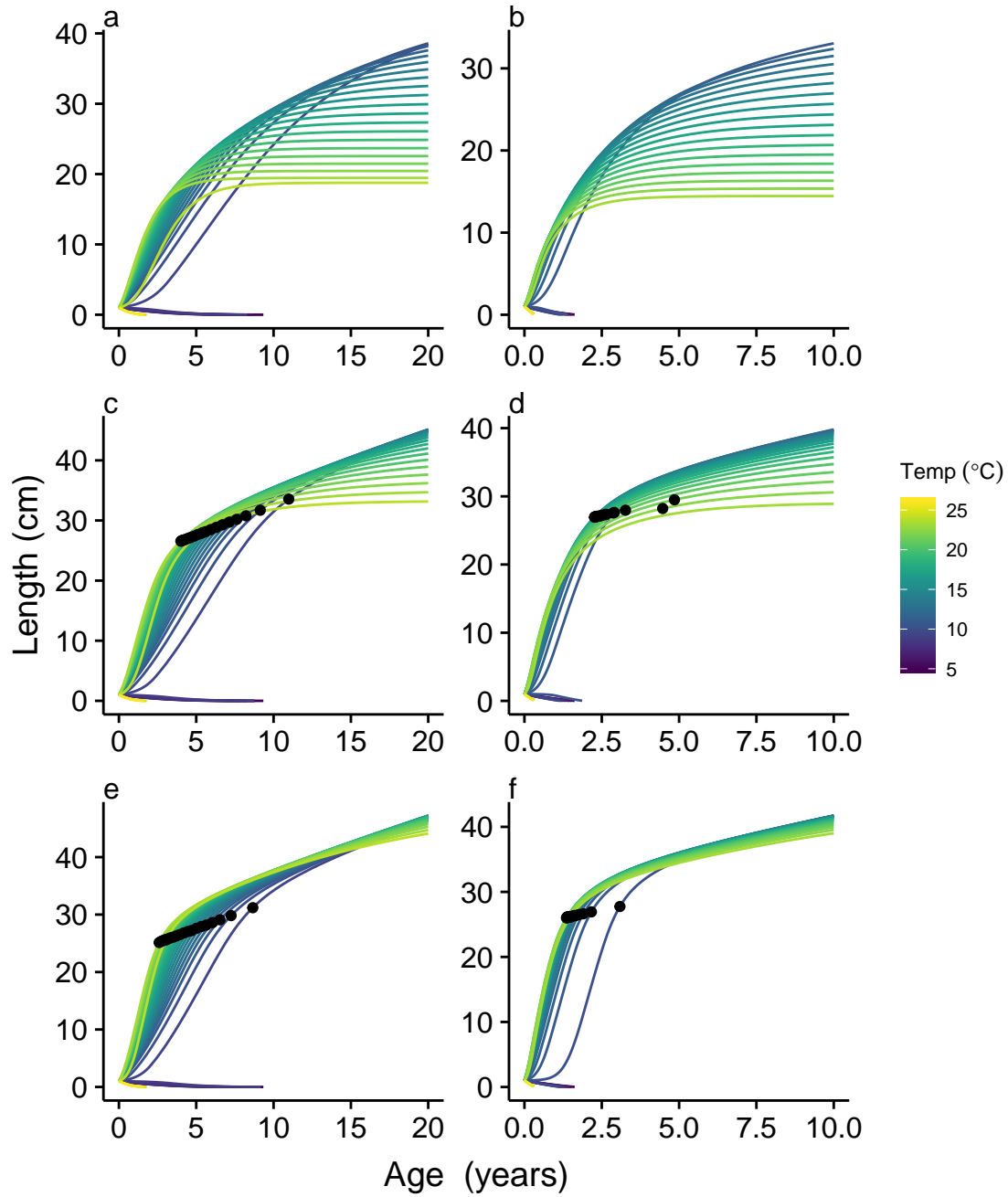
Figure S6: On ecological time-scales, increasing temperature (purple to yellow growth curves) modifies growth, and maturation age changes according to the positive reaction norm (black dots at 50% allocation to reproduction), whereas asymptotic size is affected by changes in absolute energy available for growth. Growth curves are shown for slow- (left column [a,c,e]) and fast strategists (right column [b,d,f]), at increasing food availility from top (a/b) to bottom (e/f). Baseline resource availility assumed in all other simulations is that shown in panels c and d.